Available online at www.sciencedirect.com
ScienceDirect
Journal of Molecular Catalysis A: Chemical 283 (2008) 33–42
JOURNAL OF MOLECULAR CATALYSIS A: CHEMICAL
www.elsevier.com/locate/molcata

Promotional effects of Cu and K on precipitated iron-based catalysts for Fischer–Tropsch synthesis

Haijun Wan [a,b], Baoshan Wu [a], Chenghua Zhang [a], Hongwei Xiang [a,*], Yongwang Li [a]

[a] State Key Laboratory of Coal Conversion, Institute of Coal Chemistry, Chinese Academy of Sciences, Taiyuan 030001, PR China
[b] Qingdao Institute of Biomass Energy and Bioprocess Technology, Chinese Academy of Sciences, Qingdao 266071, PR China

Received 5 November 2007; received in revised form 7 December 2007; accepted 10 December 2007
Available online 23 December 2007

Abstract

The effects of Cu and K promoters on precipitated iron-based Fischer–Tropsch synthesis (FTS) catalysts were investigated by using N_2 physical adsorption, temperature-programmed reduction/desorption (TPR/TPD) and Mössbauer effect spectroscopy (MES). The FTS performances of the catalysts were tested in a slurry-phase continuously stirred tank reactor (CSTR). The characterization results indicated that Cu promoter facilitates the high dispersion of Fe_2O_3, significantly promotes the reduction and H_2 adsorption, but severely suppresses CO adsorption and the carburization. However, K promoter severely retards the reduction and suppresses the H_2 adsorption, facilitates the CO adsorption and promotes the carburization. In the FTS reaction, it was found that Cu promoter decreases the FTS initial activity and water gas shift (WGS) reaction activity, promotes the oxidation of iron carbides to Fe_3O_4 and accelerates the deactivation of iron-based catalyst. However, K promoter improves the FTS activity and WGS reaction activity, suppresses the oxidation of iron carbide to Fe_3O_4 and significantly improves the stability of iron-based catalyst. As compared with individual promotion of Cu or K, the double promotions of Cu and K significantly improve the FTS and WGS activities and keep excellent stability. Due to weaker CO adsorption and stronger H_2 adsorption than the catalysts without Cu, Cu promoted catalysts have higher selectivity to light hydrocarbons and methane and lower selectivity to heavy hydrocarbons. However, the opposite result is obtained on the catalyst incorporated with K promoter.

Keywords: Fischer–Tropsch synthesis; Iron-based catalyst; Cu promoter; K promoter

1. Introduction

Fischer–Tropsch synthesis (FTS) has been industrialized in SASOL for almost 50 years and proved to be a promising route to meet the continuously increasing demand for liquid fuels [1,2]. Due to the excellent water gas shift (WGS) reaction activity, the use of iron-based catalyst has attracted much attention for FTS with low H_2/CO ratio synthesis gas from coal gasification [3,4]. In order to obtain excellent performances of iron-based catalyst, structural promoters are often added into the iron-based catalyst for the purpose of stabilizing small catalyst crystallites from sintering and providing the robust skeletal structure to keep the catalyst away from structure breakage during FTS reactions, especially in a slurry-phase continuously stirred tank reactor (CSTR) [5–7]. However, catalysts containing structural promoter usually suffer from lower FTS activity in the FTS reaction due to the strong metal-support interaction [8–12]. In order to improve the attrition resistance of iron-based catalysts without sacrificing their activities and selectivities, chemical promoters, such as K, Cu, Ru, Zn, etc., are often added into iron-based catalyst [13–17]. Especially, Cu and K promoters have been proved to promote the reduction of iron-based catalyst as well as the adsorption and dissociation of CO and play an important role in the FTS performances. Therefore, a large number of studies were carried out to investigate the relationship between K or Cu promoter and FTS performances of iron-based catalyst [13,14,16,17].

Miller and Moskovits [18] studied the effects of K promoter on the activity and selectivity of iron-based catalysts and found that a maximum in catalyst activity was noted upon increasing K content, followed by a sharp decline in activity at potassium levels in excess of the maximum. They also mentioned that the hydrogenation ability of the catalyst decreased, and a shift to higher molecular weight products was observed, with increasing potassium content. Bukur et al. [19] studied the

* Corresponding author. Tel.: +86 351 7560668; fax: +86 351 7560668.
E-mail addresses: haijunwan@163.com (H. Wan), hwxiang@sxicc.ac.cn (H. Xiang).

1381-1169/$ – see front matter © 2007 Elsevier B.V. All rights reserved.
doi:10.1016/j.molcata.2007.12.013

effects of K and Cu promoters on the activity and selectivity of precipitated iron-based catalysts for FTS. Their results showed that K and Cu promoters improved the FTS activity and WGS activity. They also found that K promoter enhanced the olefin and heavy hydrocarbon selectivities, whereas the addition of Cu promoter facilitated the secondary reactions (olefin hydrogenation and isomerization). Recently, Zhang et al. [14] studied the Fe–Mn catalyst promoted with Cu and found that Cu improved the rate of catalyst activation and shortened the induction period, whereas the addition of Cu has no apparent influence on the steady-state activity of iron-based catalyst. They also mentioned that the addition of Cu improved the olefin and heavy hydrocarbon selectivities due to the enhanced surface basicity.

Although K and Cu promoters have been widely used and investigated, the effects of K and Cu promoters on iron-based catalyst still keep some inconsistent conclusions, because these studies were conducted under different conditions or over different catalyst systems. Thus, there are still unabated attempts for further investigation to understand the factors what K and Cu affect the activity, selectivity and stability of iron-based catalyst. Moreover, the effects of K and Cu promoters on the stability of the active sites are rarely reported, because all these investigations were carried out in multi-component catalysts that contain other structural promoters. These structural promoters in the catalysts may significantly affect the stability of iron-based catalyst. As a result, the effect of K or Cu promoter on FTS stability could be indistinct. In order to eliminate the interference of structural promoters, four catalysts (100Fe, 100Fe/6Cu, 100Fe/5K and 100Fe/6Cu/5K) without structural promoters were prepared in this paper by using co-precipitated method to investigate the effects of K and Cu promoters on the FTS performances. Temperature-programmed reduction/desorption (TPR/TPD) and Mössbauer Effect Spectroscopy (MES) are used to elucidate how Cu and K promoters affect the reduction and carburization behaviors of iron-based catalysts. The FTS activity, stability and hydrocarbon product distribution are correlated with the catalyst characterization results.

2. Experimental

2.1. Catalyst synthesis procedure

The catalysts used in this study were prepared by a combination of co-precipitated and spray-dried method. The detailed preparation method has been described elsewhere [20–22]. In brief, a solution containing both $Fe(NO_3)_3$ and $Cu(NO_3)_2$ with a weight ratio of 100Fe/6Cu was precipitated at 80 °C using Na_2CO_3 solution. After precipitation and filtration, the precipitate was divided into two parts: one of them was added with K_2CO_3 solution in the amounts required to obtain the desired weight ratio of 100Fe/5K. The other part of precipitate was obtained with Fe/Cu ratio of 100Fe/6Cu. The Fe and Fe/K catalysts were prepared with the same method. The slurry was spray dried and then was calcined at 450 °C for 5 h. The final obtained catalysts were composed of 100Fe, 100Fe/6Cu, 100Fe/5K and 100Fe/6Cu/5K in mass ratio and shown in Table 1. These four catalysts were labeled as Fe, Fe/Cu, Fe/K and Fe/Cu/K, respectively.

Table 1
The composition and textural properties of the catalyst samples as prepared

Catalyst	Catalyst composition (parts by weight)	BET surface area (m^2/g)	Pore volume (cm^3/g)	Average pore size (nm)
Fe	Fe	28	0.21	29.84
Fe/Cu	Fe/6Cu	33	0.22	26.99
Fe/K	Fe/5K	21	0.15	28.46
Fe/Cu/K	Fe/6Cu/5K	21	0.18	33.81

2.2. Reactor system and pretreatment procedures

The FTS experiments were performed in a 1 dm^3 slurry-phase continuously stirred tank reactor (CSTR). Twenty-gram catalyst sample and 320.0 g liquid paraffin were loaded into the reactor. H_2 and CO separately passed through a serial of purified traps to remove the tiny of iron carbonyls, water and other impurities. The flow rates of H_2 and CO were controlled by two mass flow controllers (Brooks, 5850E), respectively. The exit stream passed through a hot trap (120 °C) and a cold trap (0 °C) to collect liquid products. The flow rate of the tail gas (noncondensible products and unconverted reactants) was measured by a wet gas flow meter. The catalyst was reduced in syngas (H_2/CO = 0.67) at 290 °C, 0.30 MPa and 1000 h^{-1} for 18 h. After reduction, steady-state reaction conditions were set as 260 °C, 1.5 MPa, H_2/CO = 0.67 and 1000 h^{-1}.

The tail-gas was analyzed online by an Agilent 6890N (HP) gas chromatograph (GC) with a 5A molecular sieve column (Ar carrier) and an Al_2O_3 column (N_2 carrier) equipped with a TCD and a FID. Gas components were determined by the methane concentration correlation method. CO_2 in tail gas was measured periodically on-line using an Agilent 4890D GC (HP) equipped with a TCD (H_2 carrier) and quantified by the external standard method. The oil and wax were analyzed offline using an Agilent 6890N (HP) GC with UA+-(HT) stainless steel capillary column (FID, N_2 carrier) and an Agilent 6890N (HP) GC with DB-1 quartz capillary column (FID, N_2 carrier), respectively.

2.3. Catalyst characterization equipments and procedures

The BET surface area, pore volume and average pore size were measured by N_2 physical adsorption at −196 °C using a Micromeritics ASAP 2500 instruments. The samples were degassed under vacuum at 180 °C for 6 h before measurement.

TPR experiments were performed in a quartz reactor using a mixture gas of 5% H_2/95%Ar (v/v) as the reductant. About 20 mg catalyst was packed in the quartz reactor. The catalyst sample was heated from room temperature to 800 °C at a heating rate of 6 °C/min. The flow rate of mixture gas was 50 ml/min. The hydrogen consumption was monitored by the change of thermal conductivity of the effluent gas stream.

The H_2 or CO TPD experiments were performed in the same system as used in H_2-TPR with Ar (in H_2-TPD) or He (in CO-TPD) as carrier gas. About 200 mg sample was loaded in the

reactor. It must be noted specially that, for the H_2 or CO TPD experiments, the catalyst was first reduced with H_2 or CO at 300 °C for 4 h. In the following steps, H_2 or CO adsorption on catalyst was performed at 100 °C for 30 min, and then the TPD was carried out.

The Mössbauer spectra of catalysts were recorded at room temperature using a CANBERRA Series 40 MCA constant-acceleration Mössbauer spectrometer (CANBERRA, USA), using a 25 mCi 57Co in Pd matrix. The spectrometer was operated in the symmetric constant acceleration mode. The spectra were collected over 512 channels in mirror image format. Data analysis was performed using a nonlinear least squares fitting routine that models the spectra as a combination of singlets, quadruple doublets and magnetic sextuplets based on a Lorentzian line shape profile. The spectral components were identified based on their isomer shift (δ), quadruple splitting (Δ) and magnetic hyperfine field (Hhf). All isomer shift values were reported with respect to metallic iron (α-Fe) at the measurement temperature. Magnetic hyperfine fields were calibrated with the 330 kOe field of α-Fe at ambient temperature.

3. Results and discussion

3.1. Textural properties

The surface area and pore size distribution of the fresh catalysts are shown in Table 1 and Fig. 1, respectively. It is apparent that K and Cu promoters significantly influence the surface area, pore volume and pore size distribution. Compared with Fe catalyst, Fe/Cu catalyst has larger surface area and pore volume and smaller pore size. It is probably that the addition of Cu promoter facilitates the high dispersion of the catalyst crystallites. The large surface area can be attributed to the small catalyst crystallites. The MES results in the present study also show that Fe/Cu catalyst has smaller catalyst crystallite than other catalysts. However, the addition of K promoter severely decreases the BET surface area and pore volume on Fe/K or Fe/Cu/K catalysts as compared with Fe or Fe/Cu catalysts, respectively. It may be that the addition of K promoter promotes the aggregation of the catalyst crystallites and blocks up the pore volume of the catalyst. As a synergistic effect of the results, K promoter decreases the BET surface area.

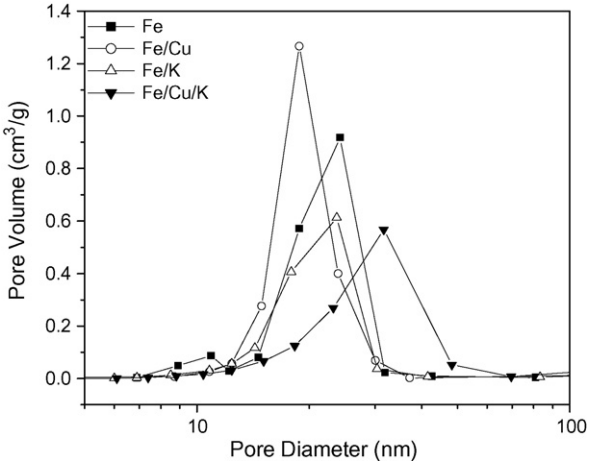

Fig. 1. The pore size distribution of the catalyst samples.

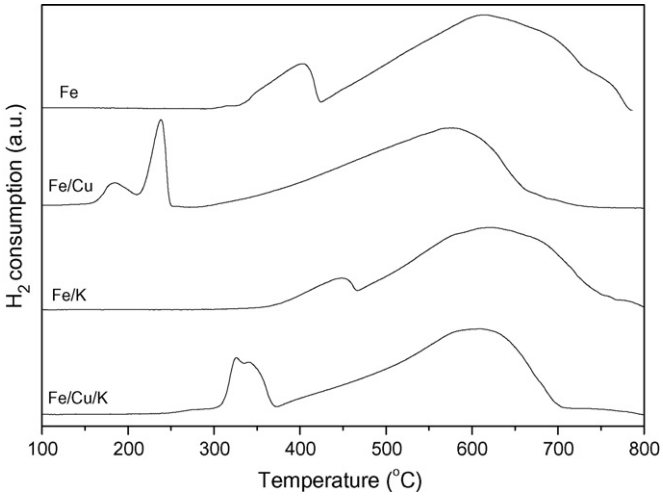

Fig. 2. H_2-TPR profiles of the catalysts.

3.2. H_2-TPR

H_2-TPR was used to investigate the effect of Cu and K promoters on the reduction behavior of the catalysts. As shown in Fig. 2, the reduction process of the catalysts occurs in two distinct stages. The first stage is ascribed to the transformations of $CuO \rightarrow Cu$ and $Fe_2O_3 \rightarrow Fe_3O_4$, whereas the second stage represents the transformation of $Fe_3O_4 \rightarrow Fe$ [4]. The H_2-TPR profiles clearly indicated that the addition of Cu significantly promotes the reduction of the two stages, whereas the addition of K promoter severely suppresses the reduction of iron-based catalyst.

It is well known that CuO is easily reduced at lower temperature in H_2 atmosphere [14,17]. As CuO reduces, Cu crystallites nucleate and provide H_2 dissociation sites, which in turn lead to reactive hydrogen species capable of reducing iron oxides at relatively low temperatures. Therefore, the addition of Cu promotes the reduction of iron-based catalyst in H_2 atmosphere. As demonstrated by H_2-TPD in the later section, the addition of K inhibits the dissociative adsorption of H_2, which suppresses the reduction of iron-based catalyst. In addition, as BET and MES results of the fresh catalysts stated in this paper, the addition of K promoter leads to the decrease in the surface area and the increase in catalyst crystallite size, which can contact with H_2 reductant; this could also contribute to the reduction phenomenon observed in Fig. 2. As a synergistic effect of the results, the reduction of iron-based catalyst in H_2 atmosphere is suppressed by addition of K promoter.

3.3. H_2-TPD

Fig. 3 shows the adsorption behavior of H_2 from the four catalysts. All of the H_2-TPD profiles have only one peak, indicating that only one type of adsorbing species could exist over

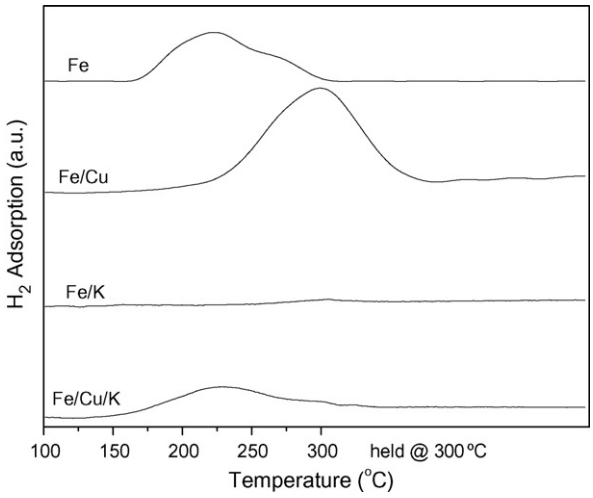

Fig. 3. H_2-TPD profiles of the catalysts.

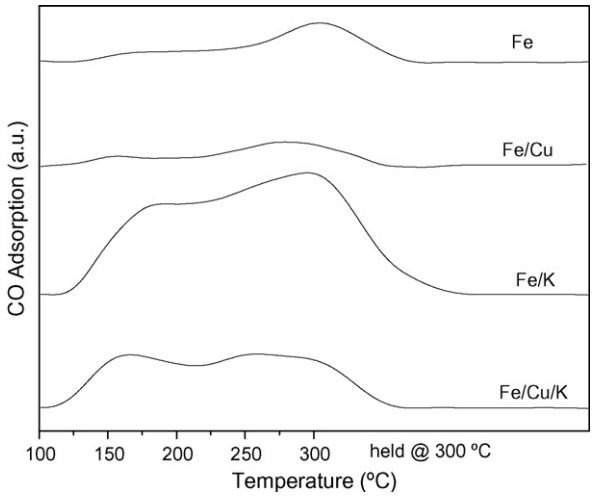

Fig. 4. CO-TPD profiles of the catalysts.

the catalysts. The desorption temperature and amount desorbed from Fe/Cu catalyst both are higher than those measured for Fe catalyst, while the addition of K promoter seriously suppresses the adsorption of H_2. Compared Fe/Cu/K with Fe/K or Fe/Cu catalyst individually, the incorporation of Cu enhances the adsorption amount of H_2, while the addition of K promoter suppresses the adsorption of H_2 and shifts the adsorption peak to lower temperature. Clearly, the addition of Cu not only leads to the large amount of H_2 adsorption, but also shifts the adsorption peak to higher temperature. However, the opposite result is obtained on the catalyst incorporated with K promoter. Previous studies [14,15] over iron-based catalysts also indicated that the incorporation of Cu into iron-based catalyst enlarges the adsorption amount of H_2 and further facilitates the reduction of iron-based catalyst. The results of H_2-TPD in present study could be attributed to that the addition of Cu promoter increases the rate of reduction of the iron oxide component in iron-based catalyst, and leads to the formation of smaller crystallites. As a result, a better dispersion of the active phase provides a greater availability of active sites for the H_2 adsorption. Therefore, the addition of Cu promoter significantly enhances the H_2 adsorption. However, K promoter has stronger surface basicity and can donate electrons to iron oxide. The electrons donated to iron oxide from K could lead to the increase in the electronic charge of the orbitals of metallic atoms. This would cause a increase in the degree of back-donating from these orbitals towards the antidonating orbitals of the chemisorbed H_2 and therefore suppress the H_2 adsorption.

3.4. CO-TPD

CO-TPD is used to investigate the effects of Cu and K promoters on the CO adsorption. As shown in Fig. 4, all catalysts have two groups of desorption peaks; one at the lower temperatures corresponding to the weak CO adsorption, while the other at higher temperatures is ascribed to the strong CO adsorption. It clearly showed that the addition of Cu promoter suppresses the CO adsorption, while the addition of K promoter promotes the CO adsorption strongly. A lot of studies had been carried out to study the effect of Cu promoter on the adsorption behavior of H_2 [14,15], whereas the effect of Cu promoter on the CO adsorption is rarely studied. As the H_2-TPD shows, Cu promoter tends to accept electrons from H_2, indicating that Cu is an electron-accepting promoter. It is well known that CO also tends to accept electrons from iron [13]. Therefore, the suppression of CO adsorption on Cu promoted iron-catalyst could be attributed to that copper accepts electrons from iron and weakens the Fe–C bond. Numerous studies have been performed to investigate the effect of K on CO adsorption over various iron-based catalysts [18,23–26]. Miller and Moskovits [18] reported that as the K level increases, the extent of CO adsorption is significantly increased. Kölbel [26] investigated the effect of K on the surface properties over supported iron and precipitated Fe–Cu–SiO_2 catalysts, and found that the addition of K promoter on the precipitated iron-based catalyst enhanced CO chemisorption and suppressed H_2 chemisorption. The results could be explained that potassium donates electrons to iron and facilitates CO chemisorption, since CO tends to accept electrons from iron. Thus the addition of K promoter facilitates the CO adsorption.

3.5. Crystallite structure of the fresh catalysts

The phase composition of the fresh catalysts is determined by MES analyses. Fig. 5 shows the Mössbauer spectra of the fresh catalysts. Table 2 lists the iron-phase composition of the fresh catalysts, as determined by fitting the Mössbauer spectra. For the catalyst samples as prepared, the content of superparamagnetic Fe^{3+} ions of Fe/Cu catalyst is higher than that of Fe catalyst, indicating that the catalyst crystallite size of Fe/Cu catalyst is smaller [14,20]. Such a result in combination with the BET surface area data indicates that the addition of Cu promoter leads to the high dispersion of catalyst crystallites [14]. Compared with Fe and Fe/Cu catalysts, respectively, the content of superparamagnetic Fe^{3+} ions of Fe/K and Fe/Cu/K catalysts is lower, indicating that the addition of K promoter do not facilitate the dispersion of iron-based catalyst [13].

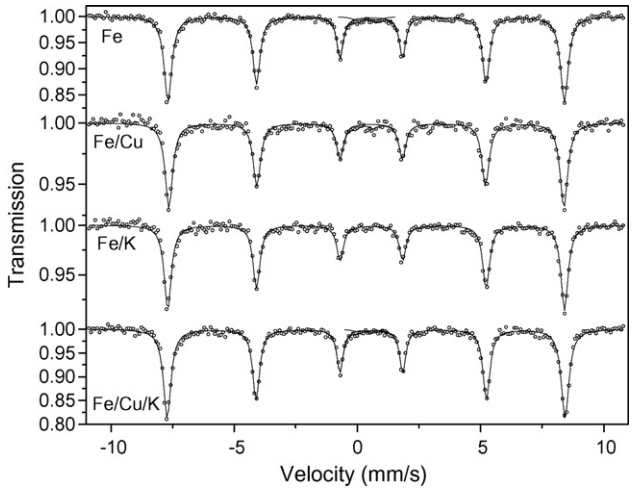

Fig. 5. Mössbauer spectra of the fresh catalysts.

Table 2
Mössbauer spectra parameters of the fresh catalysts

Catalysts	Phases	MES parameters			
		IS (mm/s)	QS (mm/s)	Hhf (kOe)	Area (%)
Fe	α-Fe_2O_3	0.46	−0.21	502	98.6
	α-Fe_2O_3 (spm)	0.32	0.70		1.4
Fe/Cu	α-Fe_2O_3	0.47	−0.19	499	97.7
	α-Fe_2O_3 (spm)	0.28	0.74		2.3
Fe/K	α-Fe_2O_3	0.46	−0.21	501	100.0
	α-Fe_2O_3 (spm)	0	0		0
Fe/Cu/K	α-Fe_2O_3	0.46	−0.21	500	98.6
	α-Fe_2O_3 (spm)	0.35	0.80		1.4

3.6. Reduction and carburization behaviors

The four catalysts were reduced in a CSTR to investigate the effects of Cu and K promoters on the reduction and carburization behaviors of iron-based catalysts. Fig. 6 shows the variation of CO_2 concentration of the catalysts in tail gas during in situ reduction. The CO_2 concentration in tail gas qualitatively reflects the reduction extent of iron-based catalyst, and thus directly reflect the reduction of the catalyst [14,15]. As shown in Fig. 6, when the temperature was increased to 290 °C and kept constant, the CO_2 concentration for Fe/Cu/K and Fe/K catalysts increased quickly to the maximum and then declined slowly with time on stream. However, those of Fe and Fe/Cu catalysts increased slowly from a low level to a high level and remained stable with increasing reduction time. It is apparent that the CO_2 concentration of Fe/Cu/K catalyst is the maximum among the four catalysts, while that of Fe/K catalyst is higher than that of Fe catalyst. The CO_2 concentration of Fe/Cu catalyst is the minimum. The results indicate that Cu promoter severely suppresses the reduction of iron-based catalyst in syngas, whereas K promoter and the double promotions of Cu and K facilitate the reduction of the catalysts in syngas.

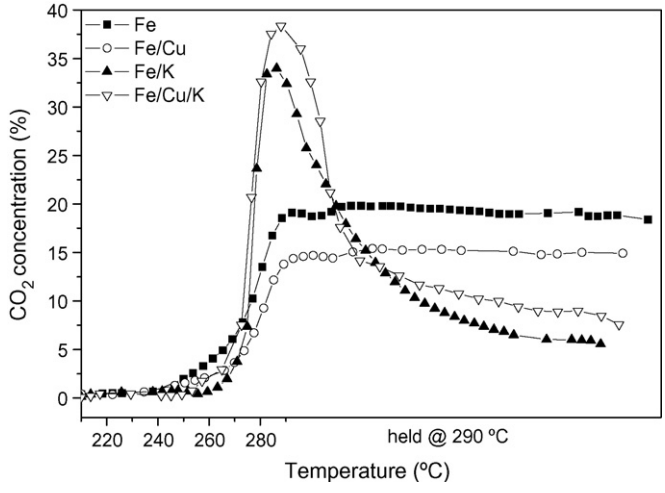

Fig. 6. The CO_2 concentration of the catalysts during in situ reduction.

Fig. 7 shows the Mössbauer spectra of the catalysts after reduction and after reaction. Table 3 lists the iron-phase composition of the catalysts, as determined by fitting the Mössbauer spectra. After reduced in synthesis gas, the content of iron carbides for Fe/Cu catalyst is the lowest during the four catalysts, whereas those for Fe/K and Fe/Cu/K are higher. The results indicate that the addition of Cu promoter suppresses the carburization of iron-based catalyst, while K promoter and the synergistic effect of Cu and K facilitate the carburization.

It is well known that the reduction of iron-based catalyst in syngas includes the removal of O (oxygen) and the introduction of C (carbon) via two steps, hematite (Fe_2O_3) to magnetite (Fe_3O_4) and magnetite to iron carbides, respectively [14]. The introduction of C into iron-based catalyst plays an important

Table 3
Iron phase composition of the catalysts at different states

Catalysts	After reduction[a]		After reaction for 200 h[b]	
	Phase	Area (%)	Phase	Area (%)
Fe	Fe_3O_4 (A)	35.1	Fe_3O_4 (A)	31.3
	Fe_3O_4 (B)	34.1	Fe_3O_4 (B)	50.4
	FeC_x	25.1	FeC_x	18.3
	Fe^{3+} (spm)	5.7	Fe^{3+} (spm)	0
Fe/Cu	Fe_3O_4 (A)	34.9	Fe_3O_4 (A)	35.2
	Fe_3O_4 (B)	34.3	Fe_3O_4 (B)	58.7
	FeC_x	21.1	FeC_x	2.9
	Fe^{3+} (spm)	9.6	Fe^{3+} (spm)	3.2
Fe/K	Fe_3O_4 (A)	0	Fe_3O_4 (A)	0
	Fe_3O_4 (B)	0	Fe_3O_4 (B)	0
	FeC_x	95.9	FeC_x	96.1
	Fe^{3+} (spm)	2.3	Fe^{3+} (spm)	1.7
	Fe^{2+} (spm)	1.8	Fe^{2+} (spm)	2.2
Fe/Cu/K	Fe_3O_4 (A)	2.4	Fe_3O_4 (A)	1.4
	Fe_3O_4 (B)	3.3	Fe_3O_4 (B)	2.3
	FeC_x	92.3	FeC_x	95.1
	Fe^{2+} (spm)	2.0	Fe^{2+} (spm)	1.2

[a] Reduction conditions: 290 °C, 0.3 MPa, $H_2/CO = 0.67$ and GHSV = 1000 h^{-1}.

[b] Reaction conditions: 260 °C, 1.5 MPa, $H_2/CO = 0.67$ and GHSV = 1000 h^{-1}.

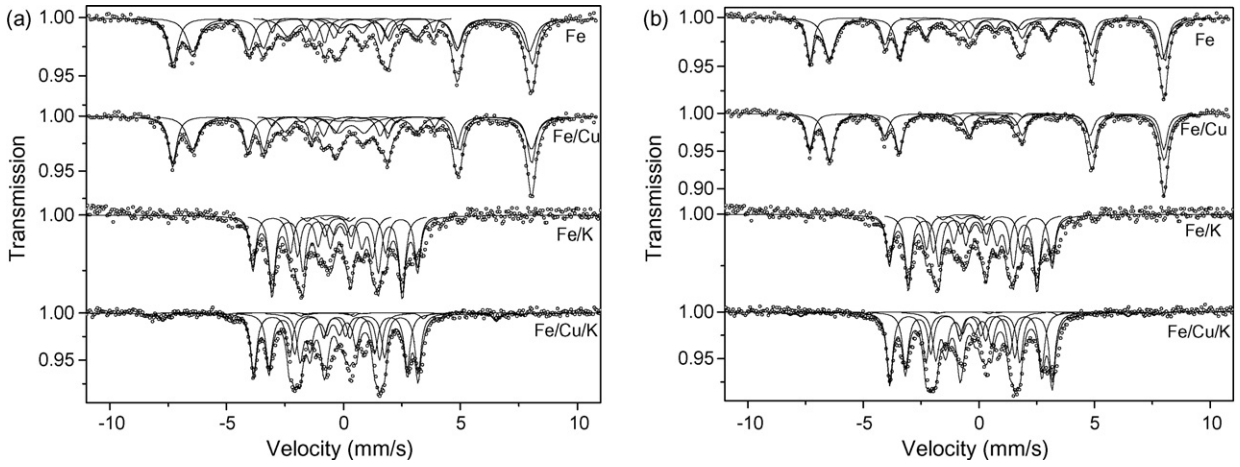

Fig. 7. Mössbauer spectra of the catalysts at different states: (a) after reduction and (b) reaction for 200 h.

role in FTS reaction. In the initial reduction stage, CuO is easily reduced to Cu, which could weaken the Fe–O bond and facilitates the removal of O. As shown by TPD, Cu promoter facilitates the adsorption of H_2, but suppresses the adsorption of CO. Although the addition of Cu promotes the reduction of $Fe_2O_3 \rightarrow Fe_3O_4$, the introduction of C into iron-based catalyst is seriously suppressed. Therefore, the content of iron carbides for reduced Fe/Cu catalyst is lower. Yang et al. [13] studied the effect of K promoter on Fe–Mn catalyst and found that K promoter suppresses the reduction of the catalyst in H_2, but facilitates the carburization of the catalyst in syngas. As TPD result shows, K promoter suppresses the adsorption of H_2, but significantly enhances the CO adsorption. During the reduction process in syngas, although K promoter prolongs the removal of O, it promotes the introduction of C and thus facilitates the carburization of the catalyst. When Cu and K promoters are incorporated into iron-based catalyst together, large amounts of K could cover the function of Cu and reduce the negative effect of Cu. Thus, the content of iron carbides for Fe/Cu/K catalyst is higher.

After reaction for 200 h, for Fe catalyst, the content of iron carbides decreases from 25.1% to 18.3%, whereas that of Fe/Cu catalyst decreases from 21.1% to 2.9% as compared with the reduced catalyst, respectively. At the same time, it should be noted that the amount of Fe_3O_4 for the two catalysts increases at different extent. The results indicate that some iron carbides of Fe catalyst are reoxidized to Fe_3O_4, whereas the addition of Cu accelerates the oxidation of $FeC_x \rightarrow Fe_3O_4$. For Fe/K and Fe/Cu/K catalysts, the content of iron carbides increases to a little extent as compared with the reduced catalysts, respectively, indicating that K promoter and double promotions of Cu and K stabilize iron carbides and suppress the oxidation of $FeC_x \rightarrow Fe_3O_4$ in the FTS reaction.

3.7. FTS performances

FTS performances of the catalysts were measured in CSTR under conditions of 260 °C, 1.5 MPa, 1000 h^{-1} and $H_2/CO = 0.67$ (v/v). The activities, stabilities and product selectivities were tested over a period of 200 h steady-state runs.

3.7.1. Activity and stability

The effects of Cu and K promoters on CO conversion are shown in Fig. 8. Fe catalyst has higher initial activity and deactivates slowly with time on stream, whereas the CO conversion of Fe/Cu catalyst is lower and deactivates quickly. The CO conversions of Fe/K and Fe/Cu/K catalysts rapidly reach a maximum and then level off. Apparently, incorporation of Cu promoter into iron-based catalyst decreases the catalyst activity and accelerates the deactivation of iron-based catalyst. The addition of K and the co-promotional effects of Cu and K not only increase the catalyst activity, but also improve the catalyst stability. It is generally accepted that the iron carbides are main active phases for the FTS reaction [17,27–30]. Thus, the content of iron carbides determined by MES can be used to monitor the amount of FTS active sites to some extent. As stated in the MES results, there is a clear correlation between the carburization extent and the catalytic activity for Fe and Fe/Cu catalysts; the higher carburization extent in the catalyst the higher CO conversion. As shown by CO-TPD, Cu promoter suppresses the adsorption of CO, then retards the carburization of the catalyst, and thus decreases the FTS activity. Fe/K and Fe/Cu/K catalysts have large amounts of iron carbides, so they have higher FTS activity. Compared Fe/K with Fe/Cu/K catalyst, it can be found that Fe/K catalyst have higher content of iron carbides than Fe/Cu/K catalyst, whereas the activity of Fe/K catalyst is lower than that of Fe/Cu/K. It seems that there is no causal relationship between the extent of carburization and the FTS activity for Fe/K and Fe/Cu/K catalysts. Miller and Moskovits [18] found that there is a competition between the dissociative adsorption of CO and H_2 on the active sites of iron-based catalysts, which results in a maximum in catalyst activity. As shown by the TPD results, K promoter significantly improves the dissoviative adsorption of CO, but severely suppresses the H_2 adsorption. Therefore, the activity of Fe/K catalyst is not higher. However, as shown by H_2-TPD, the addition of Cu promoter significantly enhances the dissociative adsorption of H_2, and the dissociative adsorption of CO is not significantly suppressed, and thus a maximum in activity is obtained on Fe/Cu/K catalyst.

As shown in Fig. 8, Fe catalyst deactivates slowly with time on stream. The addition of Cu accelerates the deactivation of

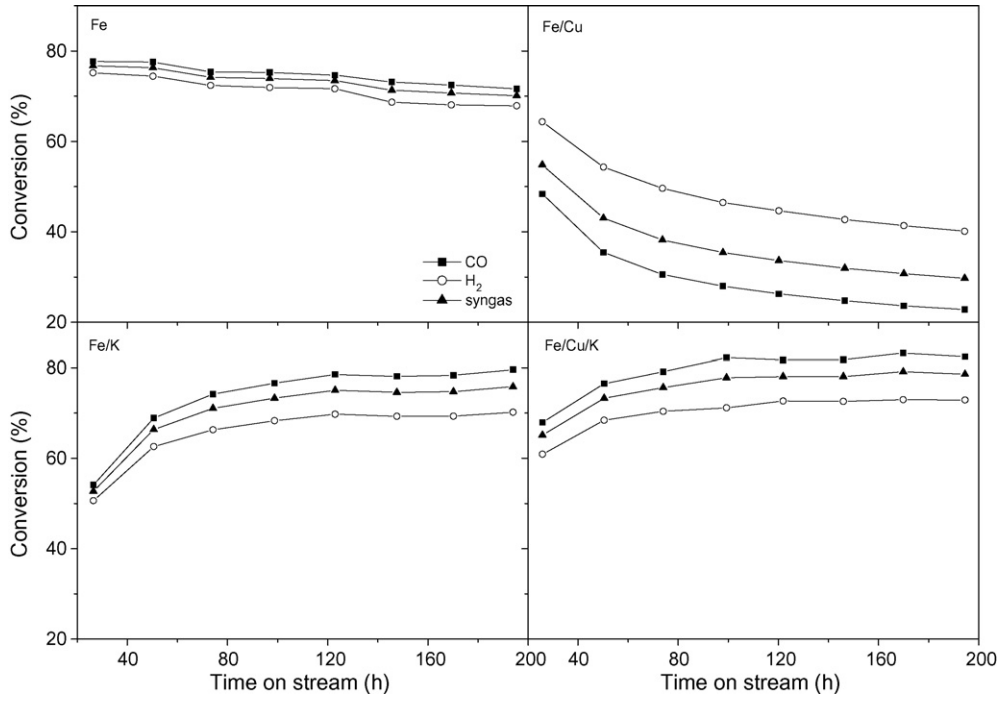

Fig. 8. The activity and stability of the catalysts. Reaction condition: 260 °C, 1.5 MPa, $H_2/CO = 0.67$ and GHSV = 1000 h^{-1}.

the catalyst, whereas the addition of K and the double promotions of Cu and K apparently improve the FTS activity of iron-based catalysts. The MES results indicate that after reaction for 200 h, the content of iron carbides for Fe and Fe/Cu catalysts decreases apparently as compared with reduced catalysts, respectively. Especially for Fe/Cu catalyst, the catalyst only has 2.9% iron carbides after reaction for 200 h. In addition, the content of Fe_3O_4 for the two catalysts increases after reaction as compared with the reduced catalyst, respectively. However, after reaction for 200 h, for Fe/K and Fe/Cu/K catalysts, the content of iron carbides do not decreases and increases slightly as compared with the reduced catalysts, respectively. The results indicate that the oxidation of $FeC_x \rightarrow Fe_3O_4$ leads to the deactivation of Fe catalyst, whereas Cu promoter accelerates the oxidation of $FeC_x \rightarrow Fe_3O_4$ and further decreases the stability of the catalyst. K promoter and the co-promotional effects of Cu and K suppress the oxidation of $FeC_x \rightarrow Fe_3O_4$ and thus improve the stability.

It has been suggested that H_2O produced by FTS reaction should be responsible for the oxidation of iron carbides [28,31–33]. Satterfield et al. [34] studied the effect of water on the iron-based catalyst for FTS in slurry phase reactor and found that the addition of water can increase the content of Fe_3O_4 and decrease the content of iron carbides and metallic iron. As a result, the catalyst deactivated quickly. They thought that H_2O plays an important role in the iron phase composition during FTS process.

It is well known that a reversible WGS reaction accompanies the FTS reaction over iron-based catalyst [13]. During FTS process, one part of H_2O produced by FTS reaction is consumed by WGS reaction, whereas the others stays in the reactor and keeps certain pressure of water vapor. Therefore, WGS reaction has an important effect on the pressure of water vapor. In other words, WGS reaction plays a significant effect on the iron phase composition.

The Q_{WGS} value and H_2/CO usage ratio are usually used as a measure of WGS activity [35,36]. The Q_{WGS} value stands for equilibrium of WGS reaction. Fig. 9 shows the Q_{WGS} value of the catalysts during FTS reaction. As shown in Fig. 9, the Q_{WGS} value of Fe/Cu catalyst is the lowest, secondly Fe and Fe/K catalysts, and that of Fe/Cu/K catalyst is the highest. The variation of H_2/CO usage ratio of the catalysts with time on stream during FTS reaction is shown in Fig. 10. The variation of H_2/CO usage ratio reflects the differences of WGS reaction. Namely, the high H_2/CO usage ratio represents lower WGS activity. As shown in Fig. 10, the H_2/CO usage ratio of Fe/Cu catalyst is the

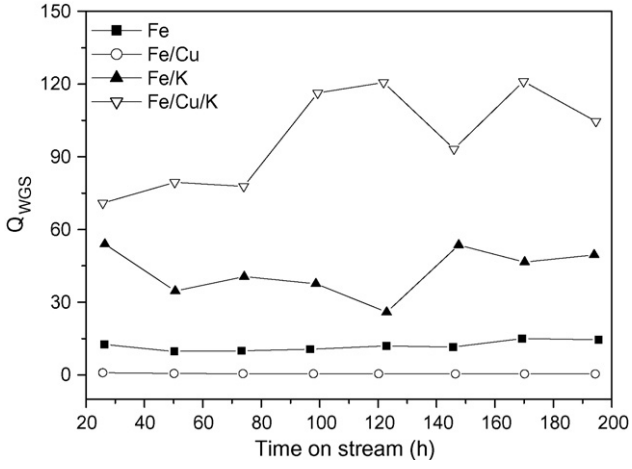

Fig. 9. The WGS activity of the catalysts during FTS reaction. Reaction condition: 260 °C, 1.5 MPa, $H_2/CO = 0.67$ and GHSV = 1000 h^{-1}.

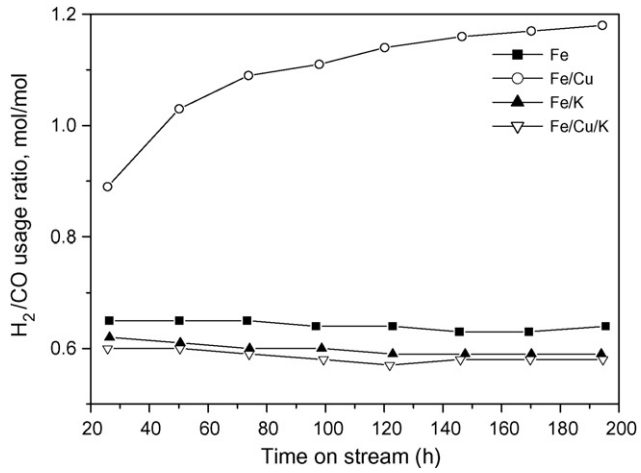

Fig. 10. The variation of H_2/CO usage ratio with time on stream during FTS reaction, conditions (as shown in Fig. 9).

highest, secondly Fe and Fe/K catalysts, and that of Fe/Cu/K is the lowest. The results of Q_{WGS} value and H_2/CO usage ratio indicate that Cu promoter suppresses WGS reaction, whereas K promoter facilitates WGS reaction. The double promotions of Cu and K significantly improve the WGS reaction activity and make Fe/Cu/K catalyst the highest WGS activity among the four catalysts.

Previous studies suggested that Fe_3O_4 could be the active sites of WGS reaction on iron-based catalyst [37], while the promoters of Cu and K are only electronic promoters. The incorporation of K promoter into iron-based catalyst can promote CO adsorption, increases the concentration of CO species, decreases the concentration of H species, shifts WGS reaction ($CO + H_2O \leftrightarrow H_2 + CO_2$) to right and thus improves WGS activity. The high WGS activity decreases the pressure of H_2O and stabilizes the iron carbides. Therefore, Fe/K catalyst has excellent stability. However, the addition of Cu promoter facilitates the adsorption of H_2, shifts the WGS reaction ($CO + H_2O \leftrightarrow H_2 + CO_2$) to left, and thus suppresses the WGS reaction. As a result, the lower WGS activity increases the pressure of H_2O and accelerates the oxidation of iron carbides. Thus, Fe/Cu catalyst deactivates quickly with time on stream. As shown in Fig. 8, the double promotions of Cu and K significantly improves the FTS activity and thus decreases the H_2/CO ratio in the reactor, whereas the Q_{WGS} value is invariable under certain conditions. As a result, the WGS reaction ($CO + H_2O \leftrightarrow H_2 + CO_2$) is shifted to right, and thus is promoted. Furthermore, the synergistic effects of Cu and K could also promote the WGS reaction [19]. Therefore, Fe/Cu/K catalyst has good stability.

3.7.2. Product selectivity

Hydrocarbon product distribution of the catalysts is shown in Table 4. It shows that Fe/Cu catalyst has the highest selectivities to gaseous and light hydrocarbons (methane, C_2–C_4 and C_5–C_{11}) and the lowest selectivities to heavy hydrocarbons (C_{12}^+ and C_{19}^+) and olefins ($C_2^=$–$C_4^=$ and $C_5^=$–$C_{11}^=$), secondly Fe and Fe/Cu/K catalysts. The selectivities to heavy hydrocarbons (C_{12}^+ and C_{19}^+) and olefins ($C_2^=$–$C_4^=$ and $C_5^=$–$C_{11}^=$) on Fe/K catalyst are the highest among the four catalysts. All of these results imply that the chain growth reaction is restrained and the hydrogenation reaction is enhanced on the catalyst incorporated with Cu promoter, whereas the addition of K promoter promotes the chain growth reaction and suppresses the hydrogenation reaction.

Both the promoters and the reaction conditions influence the product selectivity. Among all of the reaction conditions, H_2/CO ratio has the strongest influence on the production distribution [38]. Since the H_2/CO ratio in CSTR is identical with the H_2/CO ratio in tailgas, the variation of reactive H_2/CO ratio can be rep-

Table 4
The activity and selectivity of the catalysts

	Catalysts							
	Fe		Fe/Cu		Fe/K		Fe/Cu/K	
	97[a] (h)	196[a] (h)	98[a] (h)	194[a] (h)	99[a] (h)	194[a] (h)	99[a] (h)	195[a] (h)
CO conversion (%)	75.3	71.6	28.0	22.8	76.6	79.6	82.2	82.4
H_2 conversion (%)	71.9	67.9	46.5	40.1	68.3	70.2	71.2	72.9
$H_2 + CO$ conversion (%)	73.9	70.1	35.4	29.7	73.3	75.8	77.8	78.6
Exit molar H_2/CO ratio	0.76	0.76	0.50	0.52	0.91	0.98	1.1	1.0
Extent of WGS/($P_{H_2} P_{CO_2} / P_{CO} P_{H_2O}$)	13.6	14.5	0.48	0.41	47.6	49.6	116.3	104.6
Hydrocarbon selectivities (wt%)								
CH_4	8.1	8.6	12.6	11.9	3.5	3.1	4.0	4.2
C_{2-4}	10.8	10.9	21.0	17.7	4.7	4.1	5.1	5.5
C_{5-11}	25.8	25.1	45.9	47.8	20.5	18.0	21.9	22.9
C_{12-18}	35.7	36.1	19.9	21.9	26.7	27.5	24.0	26.5
C_{19}^+	19.6	19.3	0.6	0.8	44.6	47.4	45.0	41.0
CO conversion to CO_2 (mol%)	44.9	46.6	26.6	23.3	46.3	46.3	46.1	45.8
Olefin selectivity (wt%)								
$C_2^=$–$C_4^=$	66.7	66.8	67.5	66.1	79.1	77.8	77.4	77.2
$C_5^=$–$C_{11}^=$	46.9	47.8	45.5	45.5	74.5	74.3	63.0	63.3

Reaction condition: 260 °C, 1.5 MPa, H_2/CO = 0.67 and GHSV = 1000 h^{-1}.
[a] Time on stream.

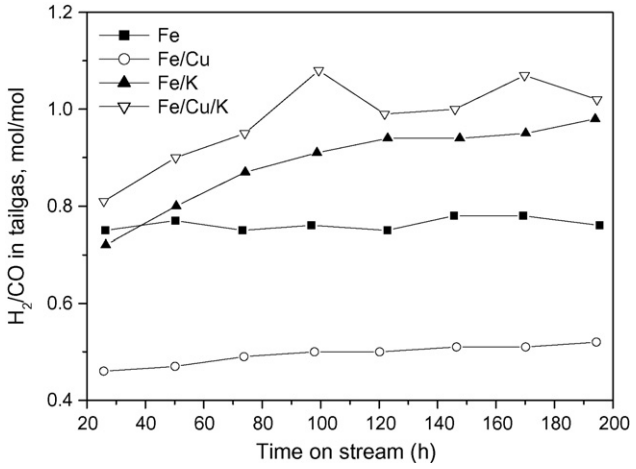

Fig. 11. The variation of H_2/CO ratio in tailgas with time on stream during FTS reaction, conditions (as shown in Fig. 9).

resent with the H_2/CO ratio in tailgas during FTS reaction. The variation of H_2/CO ratio in tailgas during FTS reaction is listed in Fig. 11. As shown in Fig. 11, the H_2/CO ratio of Fe/Cu catalyst is the lowest, secondly Fe and Fe/K, and Fe/Cu/K catalyst has the highest H_2/CO ratio. It is widely accepted that lower H_2/CO ratio should facilitate the chain growth reaction and suppress the hydrogenation reaction [14]. Therefore, Fe/Cu catalyst should have the lower selectivities to gaseous and light hydrocarbons and the higher selectivities to heavy hydrocarbons and olefin, and the opposite result should be obtained on Fe/K and Fe/Cu/K catalysts. However, the experimental results indicate that Fe/Cu catalyst has higher selectivities to gaseous and light hydrocarbons, while Fe/K and Fe/Cu/K catalysts have higher selectivities to heavy hydrocarbons and olefins. It seems that the experimental result is inconsistent with the effect of H_2/CO ratio on product selectivity. In previous section, the results have indicated that the addition of Cu and K promoters exhibit strong promotional effects, which have different effects on the product selectivity and could cover the effect of H_2/CO ratio in present study. Therefore, the opposite experimental results further reconfirmed that Cu promoter restrains the chain growth reaction and the hydrogenation reaction is suppressed by K promoter [39]. It is probably due to that Cu promoter suppresses the dissociative adsorption of CO and enhances the H_2 adsorption as shown by TPD results. Therefore, Cu promoter retards the chain propagation reaction and reduces the selectivity of olefin. However, the addition of K promoter facilitates the CO dissociative adsorption, leading to a higher coverage of carbon species on the surface and thus promotes the chain growth reaction, whereas deficient H_2 is present for the olefin production.

4. Conclusions

Incorporation of Cu and K promoters to precipitated iron-based catalyst was found to have significant influences on the adsorption, reduction and carburization behaviors, as well as catalytic performances during Fischer–Tropsch synthesis (FTS). The changes in the catalytic performances can be primarily attributed to the effects of Cu and K promoters on the H_2 adsorption and CO adsorption, which further significantly affects the FTS performances of the catalysts.

The addition of Cu promoter facilitates the high dispersion of the catalyst crystallites, significantly promotes the reduction and H_2 adsorption, but severely suppresses the carburization and CO adsorption of iron-based catalyst. However, the addition of K promoter does not facilitate the dispersion of the catalyst, severely retards the reduction and suppresses the H_2 adsorption, but facilitates the CO adsorption and significantly promotes the carburization. During FTS process, the addition of Cu promoter decreases the FTS initial activity and water gas shift reaction activity, promotes the oxidation of iron carbide to magnetite and accelerates the deactivation of iron-based catalyst. Therefore, compared with other catalysts, the catalytic stability is decreased on Fe/Cu catalyst. However, the addition of K promoter improves the FTS activity and WGS reaction activity, suppresses the oxidation of iron carbides and significantly improves the stability. As compared with individual promotion of Cu and K, the double promotions of Cu and K keep excellent stability and significantly improve the FTS and WGS activities probably due to the synergistic effects of Cu and K. Due to weaker CO adsorption and stronger H_2 adsorption than the catalyst without Cu, the chain growth reaction is restrained and the hydrogenation reaction is enhanced on the catalyst incorporated with Cu promoter. However, the addition of K promoter significantly improves the adsorption of CO, suppresses the H_2 adsorption, and thus promotes the chain growth reaction and retards the hydrogenation reaction.

Acknowledgements

We deeply appreciate the financial support from National Natural Science Foundation of China (20590361), the National Outstanding Young Scientists Foundation of China (20625620) and National Key Basic Research Program of China (973 Program, 2007CB216401). This work is also supported by Synfuels China Co., Ltd.

References

[1] V.S. Rao, G.J. Stiegel, G.J. Cinquergrane, R.D. Srivastava, Fuel Process. Technol. 30 (1992) 83.
[2] R.B. Anderson, The Fischer–Tropsch Synthesis, Academic Press, Orlando, FL, 1984.
[3] K. Jothimurugesan, J.G. Goodwin, S.K. Santosh, J.J. Spivey, Catal. Today 58 (2000) 335.
[4] Y. Jin, A.K. Datye, J. Catal. 196 (2000) 8.
[5] R. Zhao, J.G. Goodwin Jr., K. Jothimurugesan, S.K. Gangwal, J.J. Spivey, Ind. Eng. Chem. Res. 40 (2001) 1065.
[6] R.J. O'Brien, L. Xu, S. Bao, A. Raje, B.H. Davis, Appl. Catal. A: Gen. 196 (2000) 173.
[7] D.B. Bukur, C. Sivaraj, Appl. Catal. A: Gen. 231 (2002) 201.
[8] D.B. Bukur, X. Lang, D. Mukesh, W.H. Zimmerman, M.P. Rosynek, C. Li, Ind. Eng. Chem. Res. 29 (1990) 1588.
[9] A.F.H. Wielers, A.J.H.M. Kock, C.E.C.A. Hop, J.W. Geus, A.M. van der Kraan, J. Catal. 117 (1989) 1.
[10] Y. Yang, H.-W. Xiang, L. Tian, H. Wang, C.-H. Zhang, Z.-C. Tao, Y.-Y. Xu, B. Zhong, Y.-W. Li, Appl. Catal. A: Gen. 284 (2005) 105.

[11] H. Dlamini, T. Motjope, G. Joorst, G. ter Stege, M. Mdleleni, Catal. Lett. 78 (2002) 1.
[12] K.W. Jun, H.S. Roh, K.S. Kim, J.S. Ryu, K.W. Lee, Appl. Catal. A: Gen. 259 (2004) 221.
[13] Y. Yang, H.W. Xiang, Y.Y. Xu, L. Bai, Y.W. Li, Appl. Catal. A: Gen. 266 (2004) 181.
[14] C.H. Zhang, Y. Yang, B.T. Teng, T.Z. Li, H.Y. Zheng, H.W. Xiang, Y.W. Li, J. Catal. 237 (2006) 405.
[15] C. Zhang, B. Teng, Y. Yang, Z. Tao, Q. Hao, H. wan, F. Yi, B. Xu, H. Xiang, Y. Li, J. Mol. Catal. A 239 (2005) 15.
[16] H. Arakawa, A.T. Bell, Ind. Eng. Chem. Process Des. Dev. 22 (1983) 97.
[17] S. Li, S. Krisyhnamoorthy, A. Li, G.D. Meitzner, E. Iglesia, J. Catal. 206 (2002) 202.
[18] D.G. Miller, M. Moskovits, J. Phys. Chem. 92 (1988) 6081.
[19] D.B. Bukur, D. Mukesh, S.A. Patal, Ind. Eng. Chem. Res. 29 (1990) 194.
[20] H.J. Wan, B.S. Wu, C.H. Zhang, B.T. Teng, Z.C. Tao, Y. Yang, Y.L. Zhu, H.W. Xiang, Y.W. Li, Fuel 85 (2006) 1371.
[21] B. Wu, L. Bai, H. Xiang, Y.W. Li, Z. Zhang, B. Zhong, Fuel 83 (2004) 205.
[22] B. Wu, L. Tian, L. Bai, Z. Zhang, H. Xiang, Y.W. Li, Catal. Commun. 5 (2004) 253.
[23] X. Wang, G. Li, U.S. Ozkan, J. Mol. Catal. A 217 (2004) 219.
[24] M.E. Dry, G.J. Oosthuizen, J. Catal. 11 (1968) 18.
[25] J.W. Niemantsverdriet, A.M. vander Kraan, W.L. van Dijk, H.S. vander Baan, J. Phys. Chem. 84 (1980) 3363.
[26] H. Kölbel, Kalium als struktureller und Energetischer Promotor in Eisenkatalysatoren, in: Actes du Deuxieme Congress International de Catalyse, vol. II, Tchnip, Paris, 1960, p. 2075.
[27] S. Li, G.D. Meitzner, E. Iglesia, J. Phys. Chem. B 105 (2001) 5743.
[28] D.B. Buker, K. Okabe, M.P. Rosynek, C. Li, D. Wang, K.R.P.M. Rao, G.P. Huffman, J. Catal. 155 (1995) 353.
[29] T.R. Motjope, H.T. Dlamini, G.R. Hearne, N.J. Coville, Catal. Today 71 (2002) 335.
[30] L.D. Mansker, Y. Jin, D.B. Bukur, A.K. Datye, Appl. Catal. A: Gen. 186 (1999) 277.
[31] W. Ning, N. Koizumi, H. Chang, T. Mochizuki, T. Itoh, M. Yamada, Appl. Catal. A: Gen. 312 (2006) 35.
[32] D.B. Bukur, L. Nowicki, R.K. Manne, X.S. Lang, J. Catal. 155 (1995) 366.
[33] S. Li, R.J. O'Brien, G.D. Meitzner, H. Hamdeh, B.H. Davis, E. Iglesia, Appl. Catal. A: Gen. 219 (2001) 215.
[34] C.N. Satterfield, R.T. Hanlon, S.E. Tung, Z. Zou, G.C. Papaefthymiou, Ind. Eng. Chem. Prod. Res. Dev. 25 (1986) 407.
[35] H.J. Wan, B.S. Wu, C.H. Zhang, H.W. Xiang, Y.W. Li, B.F. Xu, F. Yi, Catal. Commun. 8 (2007) 1538.
[36] R.A. Dictor, A.T. Bell, J. Catal. 97 (1986) 121.
[37] R.J. Madon, W.F. Taylor, J. Catal. 69 (1981) 32.
[38] Y.Y. Ji, H.W. Xiang, J.L. Yang, Y.Y. Xu, Y.W. Li, B. Zhong, Appl. Catal. A: Gen. 214 (2001) 77.
[39] H.J. Wan, B.S. Wu, Z.C. Tao, T.Z. Li, X. An, H.W. Xiang, Y.W. Li, J. Mol. Catal. A 260 (2006) 255.